Journal of Statistical Physics, Vol. 69, Nos. 5/6, 1992

Frenkel–Kontorova Model with Toda Interactions

Bin Lin[1] **and Bambi Hu**[2]

Received March 3, 1992; final June 25, 1992

We have studied the Frenkel–Kontorova (FK) model with Toda interactions. The phase diagram is found to be asymmetric due to the exponential form of the Toda interaction. The reflection symmetry observed in the standard FK model is broken here. The singularity spectrum and the generalized dimension are calculated and their dependence on the nonlinearity parameter is discussed. The critical exponents of the gap in the phonon spectrum, the correlation length, and the Peierls–Nabarro barrier are found to be the same as those in the standard FK model and are independent of the nonlinearity parameter.

KEY WORDS: Frenkel–Kontorova model; Toda interaction; multifractal; breaking of analyticity; incommensurate.

1. INTRODUCTION

Commensurate–incommensurate phase transitions have been observed in spin- and charge-density waves,[1,2] magnetic spirals,[3] intercalation compounds,[4] and quasicrystals.[5] The Frenkel–Kontorova (FK) model[6] has been widely used to study such transitions. It is also used as a model for crystal dislocation[7] and adsorbed epitaxial monolayers.[8] This simple one-dimensional model has been proven to be most suitable for the description of various phenomena arising from competing periodicities. The Hamiltonian associated with the FK model may be written as

$$\mathscr{H} = \sum_i \left[\frac{1}{2} (x_{i+1} - x_i - \mu)^2 + \frac{k}{(2\pi)^2} (1 - \cos 2\pi x_i) \right] \tag{1}$$

[1] Department of Physics, Case Western Reserve University, Cleveland, Ohio 44106-7079.
[2] Department of Physics, University of Houston, Houston, Texas 77204-5506.

0022-4715/92/1200-1047$06.50/0

where x_i denotes the position of the ith atom and μ the length of the unperturbed spring. The second term is the external potential with strength k and period one.

In the standard FK model (1), the interatomic forces are harmonic. While interactions in some systems can be well approximated by harmonic forces, there are many systems in which the interactions are far from being harmonic. In this paper we will study a generalized FK model with anharmonic Toda interactions.[9,10] The Toda interaction $W_0(x_{i+1}-x_i)$ between two neighboring atoms is given by

$$W_0(x_{i+1}-x_i)=\frac{1}{\beta^2}\left[e^{-\beta(x_{i+1}-x_i-\mu)}-1\right]+\frac{1}{\beta}(x_{i+1}-x_i-\mu) \tag{2}$$

where β is a nonlinearity parameter measuring the degree of anharmonicity. When β tends to zero, the Toda interaction reverts to the harmonic form (standard FK model); as β increases, the interaction becomes more and more nonlinear, and in the limit $\beta\to\infty$, the Toda interaction becomes that of a hard rod:

$$\begin{aligned} &\beta\to 0, && W_0(r)\to \tfrac{1}{2}(r-\mu)^2 \\ &\beta\to\infty, && W_0(r)\to\infty \quad \text{if} \quad r<\mu \\ & && W_0(r)\to 0 \quad \text{if} \quad r\geqslant\mu \end{aligned} \tag{3}$$

where $r=x_{i+1}-x_i$.

If we consider an external cosine potential as in the standard FK model (1), the Hamiltonian for the generalized FK model with Toda interactions (2) can be written as

$$\mathcal{H}_0=\sum_i\left\{\frac{1}{\beta^2}\left[e^{-\beta(x_{i+1}-x_i-\mu)}-1\right]+\frac{1}{\beta}(x_{i+1}-x_i-\mu)+\frac{k_0}{(2\pi)^2}(1-\cos 2\pi x_i)\right\} \tag{4}$$

Milchev and Mazzucchelli[10] studied the effects of the misfit μ on the soliton description of this model. They found that the soliton picture of the dislocations breaks down beyond some critical value of the misfit. The length and the density of anharmonic solitons depend in an essential way on both the sign and the magnitude of the misfit. They also discussed the dependence of the frequency spectrum on the misfit, the nonlinear parameter β, and the external potential strength k.

In this paper we will concentrate on the phase diagram, the multifractal properties, and the critical behaviors of some physical quantities.

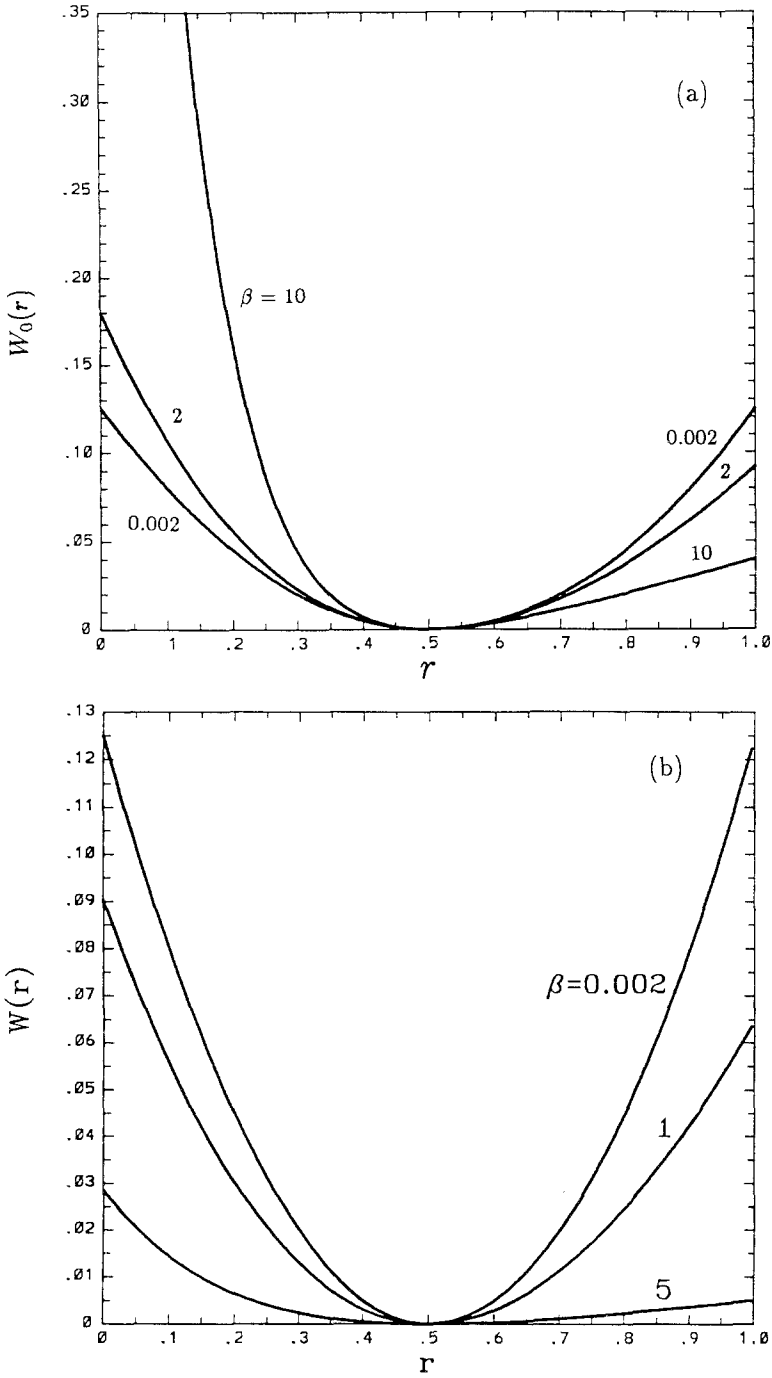

Fig. 1. Toda interaction (a) $W_0(r)$ and (b) $W(r)$ as a function of $r = x_{i+1} - x_i$ with $\mu = 0.5$ and various β.

We first rewrite the Hamiltonian (4) to rearrange the parameter μ. In Eq. (4), μ appears with the term $(x_{i+1}-x_i)$ in the exponent. This will make the boundaries of the phase diagram an implicit function and the map dependent on μ. Fortunately, we can rescale the Hamiltonian to avoid these difficulties. The new Hamiltonian $\mathscr{H}$, rescaled from $\mathscr{H}_0$ by a factor $e^{-\beta\mu}$, is given by

$$\begin{aligned}\mathscr{H} &= e^{-\beta\mu}\mathscr{H}_0 \\ &= \sum_i \left\{ \frac{1}{\beta^2}\left[e^{-\beta(x_{i+1}-x_i)} - e^{-\beta\mu}\right] \right. \\ &\quad \left. + \frac{e^{-\beta\mu}}{\beta}(x_{i+1}-x_i-\mu) + \frac{k}{(2\pi)^2}(1-\cos 2\pi x_i) \right\} \end{aligned} \tag{5}$$

where $k = e^{-\beta\mu}k_0$. In the rescaled form, the interaction $W(r) = e^{-\beta\mu}W_0(r)$ decreases monotonically as a function of β:

$$\begin{aligned} &\beta \to 0, \qquad W(r) \to \tfrac{1}{2}(r-\mu)^2 \\ &\beta \to \infty, \qquad W(r) \to 0 \end{aligned} \tag{6}$$

Figure 1 shows $W_0(r)$ and $W(r)$ for several values of β. In the following discussions we will use the rescaled Hamiltonian (5). The rest of this paper is organized as follows. The ground states and the phase diagrams will be discussed in Section 2. In Section 3 we study the devil's staircase, the singularity spectrum $f(\alpha)$, and the generalized dimension D_q. In Section 4 we compute the critical exponents of the gap in the phonon spectrum, the correlation length, and the Peierls–Nabarro barrier. Section 5 contains a brief conclusion and discussion.

2. GROUND STATE AND PHASE DIAGRAM

2.1. Ground State

Since the Toda interaction $W(r)$ is a convex function, we can use the gradient method[11–13] to calculate the periodic ground states. Consider a commensurate structure with winding number $\omega = p/q$ (the average atomic distance) defined by

$$\omega = \lim_{i-i' \to \infty} \frac{x_i - x_{i'}}{i-i'} \tag{7}$$

The initial positions of the q atoms are set up in an equal-spacing array

$$x_i(0) = i\frac{p}{q} + \alpha, \qquad i = 1, 2, \ldots, q \tag{8}$$

where the phase α, a constant throughout the system, satisfies

$$m_i \leqslant 2(i\omega + \alpha) \leqslant m_i + 1 \tag{9}$$

Here m_i is the integral part of $2x_i$:

$$m_i = [2x_i] \tag{10}$$

Let the system evolve in time according to the q differential equations

$$\frac{dx_i}{dt} = f_i, \qquad i = 1, 2, \ldots, q \tag{11}$$

where f_i is the force acting on the ith atom

$$\begin{aligned} f_i &= -\frac{\partial \mathscr{H}}{\partial x_i} \\ &= \frac{1}{\beta}\left[e^{-\beta(x_i - x_{i-1})} - e^{-\beta(x_{i+1} - x_i)}\right] - \frac{k}{2\pi}\sin 2\pi x_i, \qquad i = 1, 2, \ldots, q \end{aligned} \tag{12}$$

This evolution relaxes the system toward the ground state under the influence of the restoring forces. It has been shown[11,13] that the resulting configuration is always a ground state if the initial configuration is given by (8). A periodic condition[14] must be satisfied in Eqs. (11) and (12) to ensure periodic orbits

$$\begin{aligned} x_0 &= x_q - p \\ x_{q+1} &= x_1 + p \end{aligned} \tag{13}$$

The differential equations (11) can then be rewritten as

$$\begin{aligned} \frac{dx_1}{dt} &= \frac{1}{\beta}\left[e^{-\beta(x_1 - x_q + p)} - e^{-\beta(x_2 - x_1)}\right] - \frac{k}{2\pi}\sin 2\pi x_1 \\ \frac{dx_2}{dt} &= \frac{1}{\beta}\left[e^{-\beta(x_2 - x_1)} - e^{-\beta(x_3 - x_2)}\right] - \frac{k}{2\pi}\sin 2\pi x_2 \\ &\vdots \\ \frac{dx_{q-1}}{dt} &= \frac{1}{\beta}\left[e^{-\beta(x_{q-1} - x_{q-2})} - e^{-\beta(x_q - x_{q-1})}\right] - \frac{k}{2\pi}\sin 2\pi x_{q-1} \\ \frac{dx_q}{dt} &= \frac{1}{\beta}\left[e^{-\beta(x_q - x_{q-1})} - e^{-\beta(x_1 - x_{q-1} + p)}\right] - \frac{k}{2\pi}\sin 2\pi x_q \end{aligned} \tag{14}$$

These equations can be solved by the standard Runge-Kutta method. When the ground state is reached, the force on each atom should vanish. In practice, the ground state can be considered found if all dx_i/dt become less than a given prescribed value.

For very small values of k, the ground state is the only metastable configuration satisfying the stationary condition $\partial \mathscr{H}/\partial x_i = 0$.[11] In our calculations, for a given ω, we started with $k \to 0$, which guarantees a ground-state configuration. Then we use this configuration for the calculation of the next ground state with a small increment in k. At the same time we monitored the changes in the residue (see Section 4) to ensure that the configurations calculated stay in the minimum. If the configuration moves to a metastable state as a consequence of a small increase in k, then the residue will show a discontinuous jump from the previous value.

This method works well, but there is a practical problem. When looking for a high-period ground state, one has to integrate a large number (e.g., $q = 4181$) of differential equations simultaneously. It takes a large amount of computer time. Yet in fact, only the final configuration where all forces vanish is what we want. All the evolution steps before a ground state is reached are unnecessarily wasted. Schellnhuber *et al.*[15] suggested a Newton's method which searches directly for the solutions of $f_i = 0$. The superconvergence of Newton's method greatly reduces the computing time. Since many force functions are nonmonotonic, an extremely good guess of the correct initial condition is required in order that the method can be successfully applied. The initial condition (8) is not a good choice since very often it will converge to a physically unstable configuration for large k values. Schellnhuber *et al.* gave an optimal initial configuration for a cosine external potential such as the one we are studying:

$$x_i(0) = [ip/q] \tag{15}$$

where $[\cdot]$ stands for the integral part. The basic idea of this method is to put the atoms initially in the valleys of the potential. The system will then be trapped with certainty in the ground state before reaching a nonminimizing periodic orbit.

We compared some ground-state configurations obtained by Newton's method with the ones obtained by the differential equation method. They gave the same results, but the former method is much faster. However, caution should be exercised when applying Newton's method for other systems, since there is no guarantee that it will always result in the ground state. More complex situations have been demonstrated by Schellnhuber *et al.*[15] that a 3-harmonic external potential variant of the standard FK model also supports metastable Cantorus configurations (T-type ground

states). In the Toda model, numerical calculations of ground states showed that only the conventional on-the-bottom configurations (B-configurations) are possible.

2.2. Phase Diagram

The phase diagram consists of commensurate and incommensurate ground states in the parameter space of k and μ. For any given rational winding number ω, there is a corresponding commensurate area (Arnold's tongue) in which ω is constant. Between any two tongues there is a gap which contains incommensurate states as well as higher-order commensurate states.

The Farey tree construction[16,17] can be used to study the phase diagram from low to high orders. There are $2^{n-1}+1$ rationals (hence tongues) in the nth Farey generation in the interval $[0, 1]$. The most effective way to construct a phase diagram is to locate the boundaries of commensurate states. For a given commensurate state $\omega = p/q$, its left boundary is determined by equating the energy of that tongue to the energy of an incommensurate state $\bar{\omega}$ in the immediate left neighborhood of the tongue. Since they have the same k and μ and $\bar{\omega}$ is infinitely close to ω, their energy should also be infinitely close. In practical calculations, the incommensurate $\bar{\omega}$ is approximated by a left neighboring tongue $\bar{\omega} = \bar{p}/\bar{q}$ of a much higher order, i.e., $\bar{q} \gg q$. The higher the order, the better the approximation. We found that using $\bar{\omega}$ six orders higher than ω gives very good accuracy. The right boundary is determined in a similar way.

We divide the energy (5) into two parts:[14] the lock-in energy E_{lock} and the elastic energy E_{el}:

$$\begin{aligned}\mathscr{H} &= \sum_i \left[\frac{1}{\beta^2} e^{-\beta(x_{i+1}-x_i)} + \frac{k}{(2\pi)^2}(1-\cos 2\pi x_i) \right] \\ &\quad + \sum_i \left[\frac{e^{-\beta\mu}}{\beta}(x_{i+1}-x_i-\mu) - \frac{1}{\beta^2} e^{-\beta\mu} \right] \\ &\equiv \mathscr{H}_{\text{lock}}(\beta; \omega, k) + \mathscr{H}_{\text{el}}(\beta; \omega, \mu) \end{aligned} \tag{16}$$

where

$$\mathscr{H}_{\text{lock}}(\beta; \omega, k) = \sum_i \left[\frac{1}{\beta^2} e^{-\beta(x_{i+1}-x_i)} + \frac{k}{(2\pi)^2}(1-\cos 2\pi x_i) \right] \tag{17}$$

and

$$\mathscr{H}_{\text{el}}(\beta; \omega, \mu) = \frac{N}{\beta^2} e^{-\beta\mu}[\beta(\omega-\mu)-1] \tag{18}$$

The N in Eq. (18) is the total number of atoms in the system. The lock-in energy $\mathscr{H}_{\text{lock}}$ depends on the local atomic configurations $\{x_i\}$, and on ω

and k, but not on the parameter μ. The elastic energy $\mathscr{H}_{\text{el}}$, on the other hand, does not depend on the local properties, but only on the global properties of the system, ω and μ. A boundary μ_B of a commensurate $\omega = p/q$ at a given k is determined by the equation

$$\mathscr{H}(\beta; \omega, k, \mu_B) = \mathscr{H}(\beta; \bar{\omega}, k, \mu_B) \tag{19}$$

where $\bar{\omega} = \bar{p}/\bar{q}$ is the winding number of the neighboring tongue of a higher order. Using Eqs. (16)–(18), we can rewrite Eq. (19) to express μ_B explicitly:

$$\mu_B = \frac{1}{\beta} \ln \left[\frac{\bar{\omega} - \omega}{\beta [h_{\text{lock}}(\beta; \omega, k) - h_{\text{lock}}(\beta; \bar{\omega}, k)]} \right] \tag{20}$$

where $h_{\text{lock}}(\beta; \omega, k)$ is the average lock-in energy per atom

$$\begin{aligned} h_{\text{lock}}(\beta; \omega, k) &= \frac{1}{N} \mathscr{H}_{\text{lock}}(\beta; \omega, k) \\ &= \frac{1}{q} \sum_{i=1}^{q} \left[\frac{1}{\beta^2} e^{-\beta(x_{i+1} - x_i)} + \frac{k}{(2\pi)^2} (1 - \cos 2\pi x_i) \right] \end{aligned} \tag{21}$$

We have used the expressions (20) and (21) to calculate the phase diagrams of the model (5) for different β values (Fig. 2). Figure 2a is the phase diagram at $\beta = 0.002$, which is used as a test of the $\beta \to 0$ limit. We

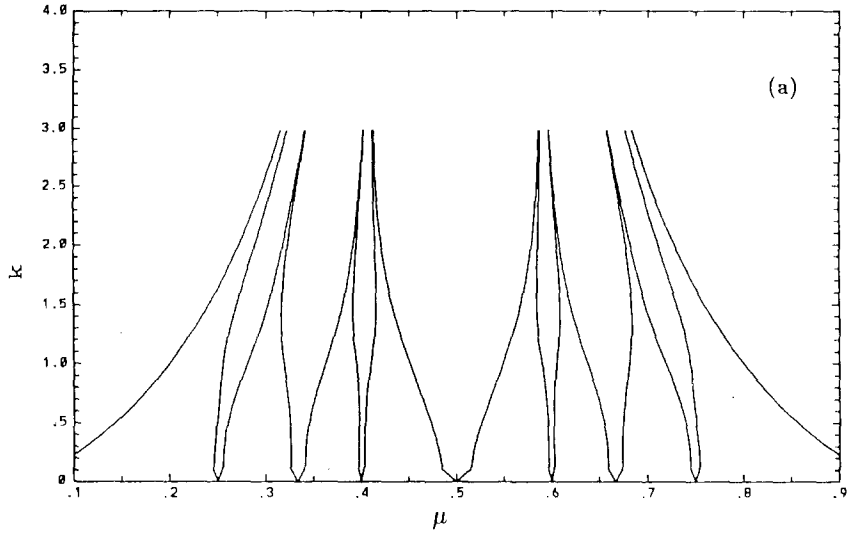

Fig. 2. Phase diagram of the FK model with Toda interactions at the fourth Farey generation. The nonsmoothness at small k values is due to the small number of data points, not a phase transition. (a) $\beta = 0.002$. The standard FK model. (b) $\beta = 2.0$. The phase diagram becomes asymmetric. (c) $\beta = 5.0$. The asymmetry becomes greater.

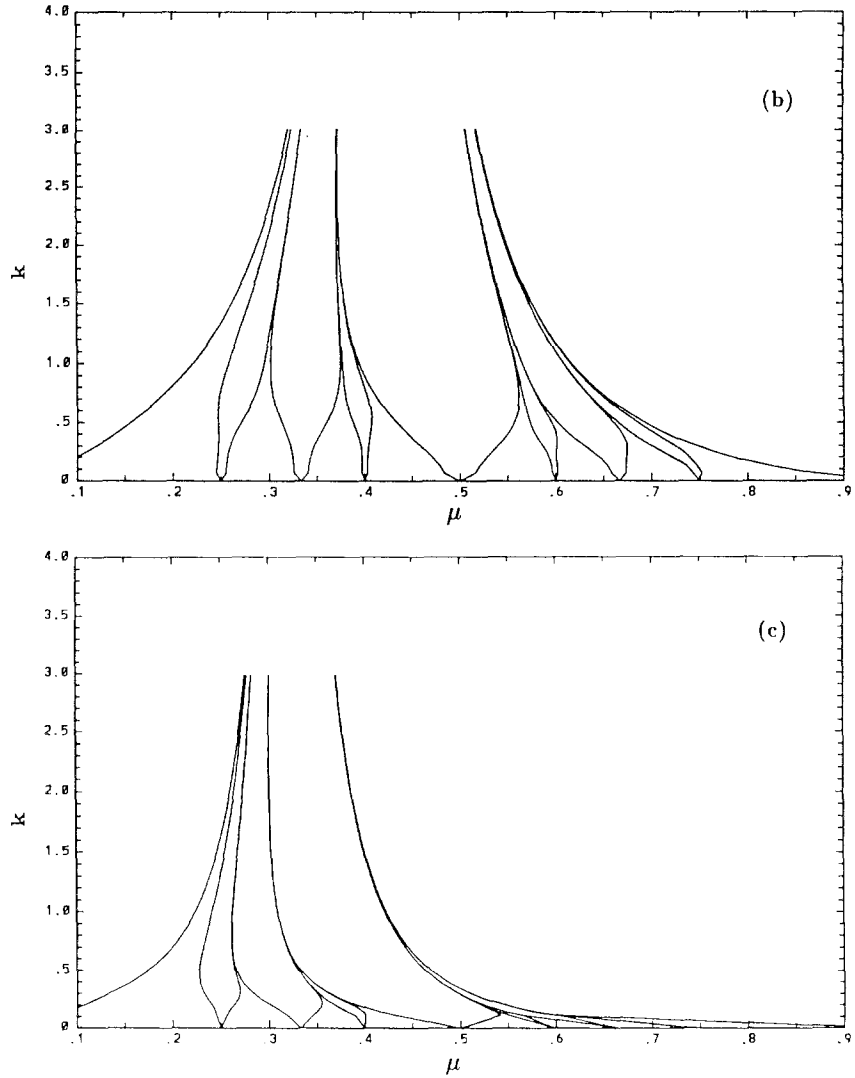

Fig. 2. (*Continued*)

can see that this phase diagram is almost the same as that of the standard FK model. It is symmetric about $\mu = 1/2$. When β is nonzero, the phase diagram becomes asymmetric (Figs. 2b and 2c), reflecting the nonlinear nature of the Toda interaction. The tongues all swing to the left. The tongues with $\mu > 1/2$ are bent more than the tongues with $\mu < 1/2$, and their areas are also reduced. The rightmost tongue, $\omega = 1/1$, becomes larger. So in our model, the small-μ part of the phase diagram remains a standard

FK type, while in the large-μ part of the diagram, the μ values are smaller compared to the standard FK model for the same stable commensurate states. As a result, the unity misfit occupies a large area in the phase diagram. For a system in which μ represents the pressure,[2,18] if the interatomic interaction is of the Toda type, then the commensurate states will occur at a lower pressure than those whose interaction is of the Hooke type. As β increases, the interaction weakens and this effect becomes greater (Figs. 1, 2b, and 2c).

3. DEVIL'S STAIRCASE, $f(\alpha)$ AND D_q

It has been shown[18,19] that on or above the critical value k_c, the frequency ratio ω as a function of the parameter μ forms a complete devil's staircase (DS) as shown in Fig. 3. This function contains only steps, each of them representing a stable commensurate state. Magnification of any part of the curve (not within a step) will reproduce the original curve. We study the devil's staircase at the critical golden mean value $k_c(\omega_G)$. The devil's staircase in Fig. 3 shows the influence of the Toda interaction: compared to the staircase of the standard FK model, the steps move to the left and get narrower as β increases. The only exception is the 1/1 step, which gets wider. The complementary set of a complete devil's staircase, namely the gaps between steps, is a fractal with zero measure. By defining a fractal measure on the fractal, we can study its multifractal properties. Consider a complete devil's staircase of the nth Farey generation. The corresponding complementary set of this staircase has 2^{n-1} pieces (gaps) in the interval $[0, 1]$. Denote by ε_i the width of the ith piece, and by m_i the fractal measure[14] defined to be the difference of the winding numbers of two neighboring steps:

$$m_i = \omega_{i+1} - \omega_i, \qquad i = 1, 2, \ldots, 2^{n-1} \tag{22}$$

Thus m_i satisfies the normalization condition

$$\sum_i m_i = 1 \tag{23}$$

The partition function[20] of this multifractal in the nth Farey generation is then

$$\Gamma^{(n)}(q, \tau) = \sum_{i=1}^{2^{n-1}} \frac{m_i^q}{\varepsilon_i^\tau} \tag{24}$$

The function $\tau(q)$ can be obtained by equating (24) to a finite constant C. We choose $C = 1$. Then $\tau(q)$ is defined by

$$\sum_{i=1}^{2^{n-1}} \frac{m_i^q}{\varepsilon_i^{\tau(q)}} = 1 \tag{25}$$

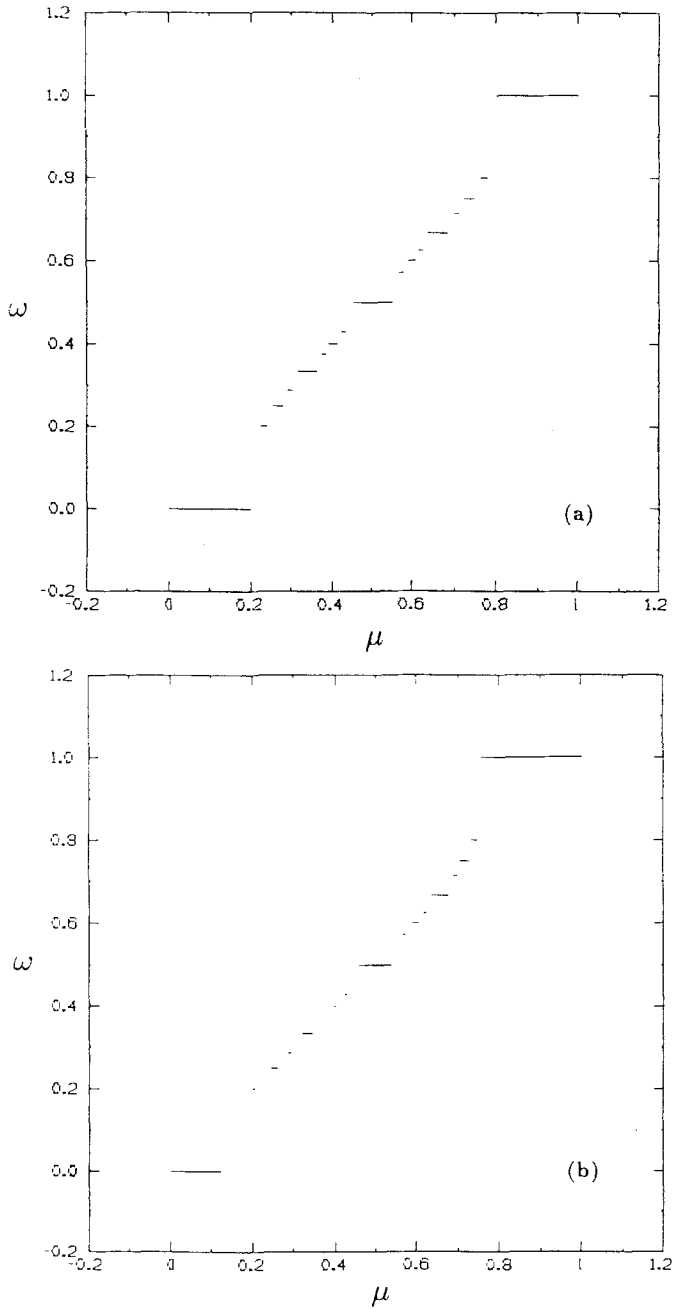

Fig. 3. Complete devil's staircase of the FK model with Toda interactions. Staircases up to the fifth Farey generation are shown. (a) $\beta = 0.002$. The standard FK model. (b) $\beta = 2.0$.

$\alpha(q)$ is defined to be the derivative of $\tau(q)$,

$$\alpha(q) = \frac{d}{dq}\tau(q) \tag{26}$$

Hence

$$\alpha(q) = \left(\sum_i \frac{m_i^q}{\varepsilon_i^\tau} \ln m_i\right) \Big/ \left(\sum_i \frac{m_i^q}{\varepsilon_i^\tau} \ln \varepsilon_i\right) \tag{27}$$

The singularity spectrum $f(\alpha)$ and the generalized dimension D_q can then be calculated:

$$f(\alpha) = q\alpha(q) - \tau(q) \tag{28}$$

$$D_q = \frac{\tau(q)}{q-1} \tag{29}$$

We have calculated $f(\alpha)$ and D_q of the devil's staircase for different β values. The numerical results are shown in Figs. 4 and 5. The singularity spectrum $f(\alpha)$ shows its dependence on the parameter β. It becomes higher as β increases. This is due to the fact that the devil's steps decrease as β

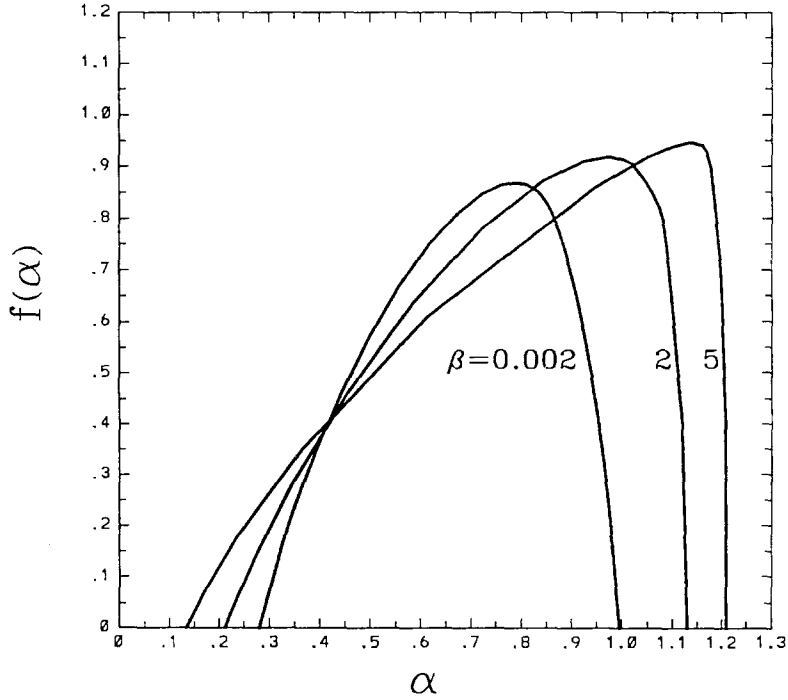

Fig. 4. Singularity spectrum $f(\alpha)$ of the complete devil's staircase with various β.

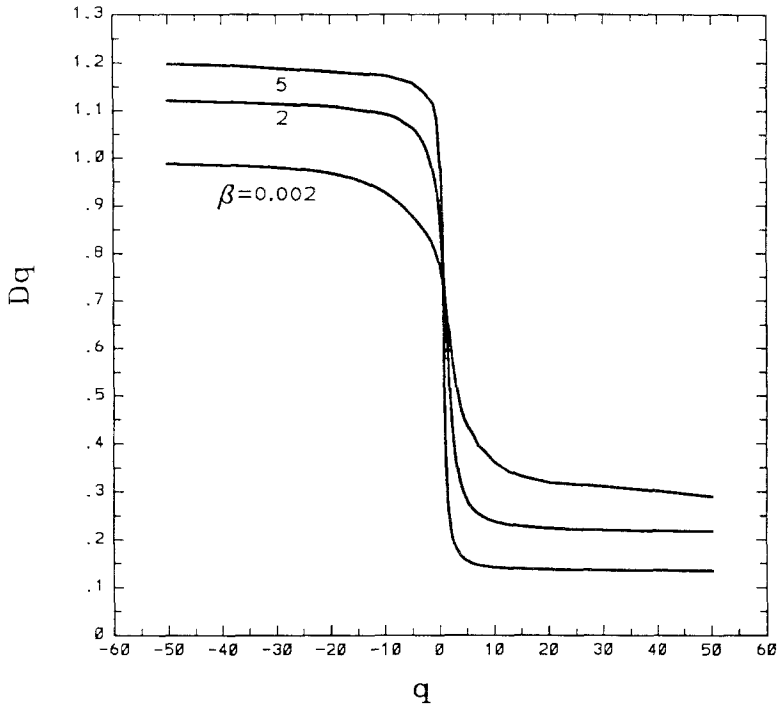

Fig. 5. Generalized dimension D_q of the complete devil's staircase with various β.

increases, causing the fractal dimension of the fractal support to increase. The endpoints of the curve, $\alpha_{\min}$ and $\alpha_{\max}$ (corresponding to $q \to +\infty$ and $q \to -\infty$, respectively), also expand as β increases: $\alpha_{\min}$ smaller and $\alpha_{\max}$ larger. The peak of the curve, α_0, shifts to the right as β increases, making the large-α side of the curve steeper. In the limit $\beta \to \infty$, $f(\alpha)$ will have a sawtooth shape, $\alpha_0 = \alpha_{\max}$. The change of the generalized dimension D_q with parameter β is shown in Fig. 5. A larger β gives a D_q curve with a higher kink.

4. CRITICAL BEHAVIOR

4.1. Map and Critical Point

The equilibrium configuration of the Hamiltonian (5) can be expressed as a map. The equilibrium configuration of the atoms is achieved by the zero-force condition:

$$\frac{\partial \mathcal{H}}{\partial x_i} = 0 \tag{30}$$

Define the conjugate variable y_i,

$$y_i = e^{-\beta(x_i - x_{i-1})} \tag{31}$$

Then condition (30) can be written in terms of a map:

$$\begin{aligned} y_{i+1} &= y_i - \frac{\beta k}{2\pi} \sin 2\pi x_i \\ x_{i+1} &= x_i - \frac{1}{\beta} \ln y_{i+1} \end{aligned} \tag{32}$$

When k is small, there are KAM curves in the (x, y) phase space. The last rotational KAM curve corresponding to the one with the golden mean winding number breaks up at $k = k_c$, and the analytic KAM curve becomes a Cantorus.

To study the critical behavior, we first have to locate the critical point k_c. We will use Greene's residue criterion[21,22] to determine the critical point. Denote by $R_i^e(k)$ and $R_i^h(k)$ the residues of the elliptic and hyperbolic orbits with period q_i. The rational approximation of the golden mean winding number is given by the convergents p_i/q_i,

$$\omega_G = \lim_{i \to \infty} \frac{p_i}{q_i} = \lim_{i \to \infty} \frac{F_i}{F_{i+1}} \tag{33}$$

where the numbers F_i define a Fibionacci sequence $F_{i+1} = F_i + F_{i-1}$ with $F_0 = 1$ and $F_1 = 1$. The residue criterion states

$$\lim_{i \to \infty} R_i^e(k) = \begin{cases} 0^+ & k < k_c \\ a & k = k_c \\ \infty & k > k_c \end{cases} \tag{34a}$$

$$\lim_{i \to \infty} R_i^h(k) = \begin{cases} 0^- & k < k_c \\ -b & k = k_c \\ -\infty & k > k_c \end{cases} \tag{34b}$$

where a and b are positive constants less than unity. The residue R is defined via the Jacobian matrix M of the linearized map (32):

$$\begin{pmatrix} \delta y_{i+1} \\ \delta x_{i+1} \end{pmatrix} = M_i \begin{pmatrix} \delta y_i \\ \delta x_i \end{pmatrix} \tag{35}$$

where

$$M_i = \begin{pmatrix} 1 & -\beta k \cos 2\pi x_i \\ -\dfrac{1}{\beta y_{i+1}} & 1 + \dfrac{k \cos 2\pi x_i}{y_{i+1}} \end{pmatrix} \tag{36}$$

For a q-orbit, M is given by

$$M = \prod_{i=1}^{q} M_i \tag{37}$$

The residue R of that orbit is defined by[21]

$$R = \tfrac{1}{4}(2 - \operatorname{Tr} M) \tag{38}$$

To calculate k_c, we use the map combined with Newton's method to reduce the computing time. The symmetry lines greatly simplify the searching for periodic orbits in the (x, y) space. The map (32) has four symmetry lines:

$$\begin{aligned} x &= 0 \\ x &= \frac{1}{2} \\ x &= -\frac{1}{2\beta} \ln y \\ x &= \frac{1}{2} - \frac{1}{2\beta} \ln y \end{aligned} \tag{39}$$

It has been observed[21,23] that for a q-orbit there are at least two out of its q points which lie on the symmetry lines. The search for a q-orbit is then limited to these four lines instead of the whole (x, y) space.

We have calculated the k_c values of the golden mean winding number ω_G for different β values. Table I lists the numerical values of k_c.[3] Also

[3] Some of the k_c were provided by J. Shi.

Table I. Critical Point k_c with Winding Numbers ω_G and $\omega_{\bar{G}}$ for Various β

β	$k_c(\omega_G)$	$k_c(\omega_{\bar{G}})$
0.0	0.971635	0.971635
0.002	0.970473	0.970842
0.1	0.915184	0.933420
1.0	0.534561	—
2.0	0.294788	0.437262
5.0	0.0502393	—
10.0	0.00284025	—

listed are $k_c(\omega_{\bar{G}})$, where $\omega_{\bar{G}} = 1 - \omega_G$ for some selected β values. At $\beta = 0$, which is the standard FK model, $k_c(\omega_G) = k_c(\omega_{\bar{G}})$. But $k_c(\omega_G)$ and $k_c(\omega_{\bar{G}})$ become distinct as $\beta \neq 0$, and their difference increases as β increases. This reflects the asymmetry of the map (32). For the standard FK model, its map, the standard map,

$$y_{i+1} = y_i + \frac{k}{2\pi} \sin 2\pi x_i$$

$$x_{i+1} = x_i + y_{i+1}$$

is invariant under the interchange of ω and $1 - \omega$, i.e., $y \to 1 - y$. The map (32) of the Toda interaction does not have this symmetry, due to the exponential form of the Toda interaction (logarithm term in the map). As a result, the k_c values for ω_G and $\omega_{\bar{G}}$ become unequal. However, we will see in the next section that the critical exponents at $k_c(\omega_G)$ and $k_c(\omega_{\bar{G}})$ are nevertheless identical.

4.2. Critical Exponents

At the critical point $k = k_c$, there is a transition by breaking of analyticity.[11] The full function describing the incommensurate structure undergoes a transition from an analytic function to a discontinuous function. Many physical quantities[11] also undergo a transition at k_c. We will study their critical behavior in our model.

First consider the gap in the phonon spectrum Ω_G. Consider a small vibration of the atoms around their equilibrium positions $\{x_i\}$,

$$x_i(t) = x_i + \varepsilon_i(t) \tag{40}$$

The equation of motion for this vibration is described by

$$\frac{d^2 x_i(t)}{dt^2} = -\frac{\partial \mathscr{H}(\{x_i(t)\})}{\partial x_i(t)} \tag{41}$$

Since the equilibrium positions $\{x_i\}$ are determined by the condition

$$\left.\frac{\partial \mathscr{H}(\{x_i(t)\})}{\partial x_i(t)}\right|_{x_i(t) = x_i} = 0 \tag{42}$$

the linearized equation of motion for small vibrations is given by

$$\delta \ddot{x}_i(t) + \sum_j \frac{\partial^2 \mathscr{H}(\{x_i(t)\})}{\partial x_i(t)\, \partial x_j(t)} \delta_j(t) = 0, \qquad i = 1, 2, \ldots, q \tag{43}$$

where $\ddot{x} = d^2x/dt^2$ and

$$\frac{\partial^2 \mathscr{H}}{\partial x_i \, \partial x_j} = \begin{cases} -e^{-\beta(x_{i+1}-x_i)}, & j = i+1 \\ e^{-\beta(x_{i+1}-x_i)} + e^{-\beta(x_i - x_{i-1})} + k\cos 2\pi x_i, & j = i \\ -e^{-\beta(x_i - x_{i-1})}, & j = i-1 \end{cases} \tag{44}$$

A time Fourier transform of Eq. (43) gives

$$\begin{aligned} -e^{-\beta(x_i - x_{i-1})}\varepsilon_{i-1} + [e^{-\beta(x_{i+1}-x_i)} + e^{-\beta(x_i - x_{i-1})} + k\cos 2\pi x_i - \Omega^2]\,\varepsilon_i \\ - e^{-\beta(x_{i+1}-x_i)}\varepsilon_{i+1} = 0, \qquad i = 1, 2, \ldots, q \end{aligned} \tag{45}$$

Define two functions $D(x_{i+1}, x_i, x_{i-1})$ and $N(x_i, x_{i-1})$:

$$D(x_{i+1}, x_i, x_{i-1}) = e^{-\beta(x_{i+1}-x_i-\mu)} + e^{-\beta(x_i - x_{i-1})} + k\cos 2\pi x_i \tag{46}$$

$$N(x_i, x_{i-1}) = -e^{-\beta(x_i - x_{i-1})} \tag{47}$$

Then the eigenvalue equation (45) can be written as

$$\begin{pmatrix} D(x_2, x_1, x_0) - \Omega^2 & N(x_2, x_1) & 0 & \cdots & N(x_1, x_0) \\ N(x_2, x_1) & D(x_3, x_2, x_1) - \Omega^2 & N(x_3, x_2) & \cdots & 0 \\ 0 & N(x_3, x_2) & D(x_4, x_3, x_2) - \Omega^2 & \cdots & 0 \\ & & \vdots & & \\ N(x_{q+1}, x_q) & 0 & 0 & \cdots & D(x_{q+1}, x_q, x_{q-1}) - \Omega^2 \end{pmatrix} = 0 \tag{48}$$

with the periodic boundary condition (13).

The phonon spectrum $\{\Omega_i\}$ is obtained by solving this $q \times q$ matrix equation. The gap in the phonon spectrum Ω_G is defined to be the lowest phonon frequency in the system, $\Omega_G = \min\{\Omega_i\}$. For $k < k_c$, the ground state of the chain is in a sliding mode and the atomic positions can be described by a hull function[18] h

$$x_i = h(i\omega + \alpha) = i\omega + \alpha + g(i\omega + \alpha) \tag{49}$$

where α is an arbitrary phase. g is a continuous periodic function with the same period as the external potential. Since the hull function is analytic for $k < k_c$, we can substitute Eq. (49) for x_i in Eq. (42) and differentiate Eq. (42) with respect to the phase α,

$$\begin{aligned} -e^{-\beta(x_i - x_{i-1})}h'_{i-1} + [e^{-\beta(x_{i+1}-x_i)} + e^{-\beta(x_i - x_{i-1})} + k\cos 2\pi x_i]\,h'_i \\ - e^{-\beta(x_{i+1}-x_i)}h'_{i+1} = 0, \qquad i = 1, 2, \ldots, q \end{aligned} \tag{50}$$

where $h_i' = (\partial/\partial\alpha)\, h(i\omega + \alpha)$. The Fourier transform of (50) shows that $h_i'(\omega)$ is a solution of Eq. (45) with $\Omega = 0$. Therefore $\Omega_G = 0$ for $k < k_c$. As $k > k_c$, a gap Ω_G in the phonon spectrum appears and the critical behavior of Ω_G can be characterized by the exponent[11] χ

$$\Omega_G(k) \sim (k - k_c)^{\chi} \tag{51}$$

We have calculated χ for various β values, from $\beta = 0.002$ up to $\beta = 10$. Despite the fact that k_c increases more than two orders in this β range and the phase diagram changes greatly, χ remains unchanged. Our numerical estimate of χ is

$$\chi = 1.02 \pm 0.01 \tag{52}$$

The χ value for ω_G is found to be the same as that for ω_G. We next study the critical behavior of the correlation length.

The correlation length ξ measures the distance over which a perturbation δx_i propagates along the chain. An infinitesimal displacement δx_i at x_i will cause a displacement δx_j at x_j, where

$$\delta x_j \sim \exp(-|j - i|/\xi)\, \delta x_i \tag{53}$$

The relation (53) defines the correlation length of the ground state. It can be shown[11] that ξ is the inverse of the Lyapunov exponent γ,

$$\xi = \frac{1}{\gamma} \tag{54}$$

ξ and γ thus share the same critical exponent ν. We will use γ to calculate the exponent ν. The Lyapunov exponent can be calculated from the eigenvalue of the Jacobian matrix M, (37):

$$\gamma = \lim_{q \to \infty} \frac{1}{q} \ln |\lambda_l| \tag{55}$$

where $|\lambda_l|$ is the modulus of the larger eigenvalue of M, and q is the period of the orbit. The eigenvalue λ of the matrix M can be expressed in terms of its trace Tr M,

$$\lambda_{\pm} = \frac{1}{2} \operatorname{Tr} M \left\{ 1 \pm \left[1 - \left(\frac{2}{\operatorname{Tr} M} \right)^2 \right]^{1/2} \right\} \tag{56}$$

In the sliding mode $k < k_c$, $\xi \to \infty$ since the chain can slide freely under an infinitesimal displacing force. For $k > k_c$, the atoms are locked, ξ is

therefore finite, and so is γ. The critical exponent ν describes the critical behavior of γ:

$$\gamma(k) \sim (k - k_c)^{\nu} \tag{57}$$

As in the case of χ, the values of ν for various β are all the same. We calculated ν for β from 0.002 to 10, and found no appreciable difference. Also, the value of ν at $k_c(\omega_{\bar{G}})$ is the same as that at $k_c(\omega_G)$:

$$\nu = 0.99 \pm 0.01 \tag{58}$$

The Peierls–Nabarro (PN) barrier of the ground state is defined to be the minimal energy barrier that must be overcome to continuously translate the chain of atoms on the external potential. For $k < k_c$, the PN barrier E_{PN} vanishes since no extra energy is needed to shift the chain in this sliding mode. For $k > k_c$, the ground state is described by a discontinuous hull function which in the (x, y) phase space is represented by a Cantor set. A minimizing periodic orbit $\{(y_i, x_i)\}_{i=1}^{q}$ can be used to approximate this Cantor set.[24] The PN barrier E_{PN} is the energy difference between the minimizing orbit and its companion minimax orbit,

$$E_{\mathrm{PN}} = E_{\max}(\omega) - E_{\min}(\omega) \tag{59}$$

where $E_{\max}(\omega)$ $[E_{\min}(\omega)]$ is the energy of the minimax (minimizing) orbit of winding number ω. The critical behavior of E_{PN} obeys the following power law:

$$E_{\mathrm{PN}} \sim (k - k_c)^{\psi} \tag{60}$$

The critical exponent ψ is found to be

$$\psi = 3.00 \pm 0.02 \tag{61}$$

for all β values we have calculated, ψ is also the same for $k_c(\omega_G)$ and $k_c(\omega_{\bar{G}})$. The scaling law observed in ref. 11 also holds in the FK model with Toda interactions

$$\psi = 2\chi + \nu \tag{62}$$

Since all the critical exponents we have calculated are the same for the standard FK model and the FK model with Toda interactions, these two models belong to the same universality class in the conventional sense.

Recently, MacKay[25] used the renormalization theory to study the critical exponents and the scaling law. He predicted that the scaling law (62) should be corrected as

$$\psi + \eta' = 2\chi + \nu \tag{63}$$

where η' is the critical exponent for the effective mass m^*,

$$m^*(k) \sim (k - k_c)^{-\eta'} \tag{64}$$

with the estimated value[19] $\eta' \approx 0.029$. The effective mass m^* results from the dynamical problem

$$m_0 \ddot{x}_i(t) = -\frac{\partial \mathscr{H}(x_i(t))}{\partial x_i(t)} \tag{65}$$

The kinetic energy per atom is $(1/2)\, m^* v^2$ for small v, where the effective mass m^* is given by

$$m^* = m_0 \int_s g'^2(s)\, ds \tag{66}$$

$g(s)$ in Eq. (66) is an adiabatic solution of Eq. (65),

$$x_i(t) = g(x_0 + vt + i\omega) \tag{67}$$

5. CONCLUSIONS AND DISCUSSIONS

We have studied a strongly nonlinear system: the FK model with Toda interactions. With an adjustable nonlinearity parameter β, this model covers various types of systems: from the standard FK model as $\beta \to 0$, with stronger anharmonic interaction as β increases, to the hard-rod model as $\beta \to \infty$. A number of new features appear due to the exponential form of the Toda interaction. The phase diagram becomes asymmetric when $\beta \neq 0$, which reflects the breaking of reflection symmetry presented in the standard FK model. This asymmetry increases with β. The singularity spectrum $f(\alpha)$ and the generalized dimension D_q also show their dependence on β. In particular, the fractal dimension of the support increases as β increases. In the hard-rod limit, $f(\alpha)$ has a sawtooth shape. This shows that the multifractal feature of the Toda model is different from that of the standard FK model. The Toda interaction also destroys the symmetry of $\omega \to 1 - \omega$ in the map of the standard FK model. As a result, the critical k_c values at ω_G and $\omega_{\bar{G}} = 1 - \omega_G$ are distinct and they are functions of β.

To answer the question of whether the critical exponents of the transition by breaking of analyticity in an anharmonic FK model are different from those of the standard FK model, we have calculated the critical exponents of the gap in the phonon spectrum, the correlation length, and the Peierls–Nabarro barrier at $k_c(\omega_G)$ and $k_c(\omega_{\bar{G}})$ with different β values. Contrary to the multifractal properties, these critical exponents are the

same in the two systems. On the other hand, the critical exponents are found to be different for external potentials different from the standard cosine.[26,27] These results seem to suggest that different interatomic interactions lead to the same critical exponents, while different external potentials lead to different critical exponents.

In our calculations of $f(\alpha)$ and the critical exponents, $k_c(\omega_G)$ was used as the critical point. While $k_c(\omega_G)$ is indeed the largest $k_c(\omega)$ in the standard FK model (corresponding to the standard map), it is not the case for Toda interactions. As we have seen, $k_c(\omega_{\bar{G}})$ is greater than $k_c(\omega_G)$ for nonzero β, and the difference increases with β. Yet $k_c(\omega_{\bar{G}})$ is still not necessarily the largest $k_c(\omega)$. In principle, one needs to calculate k_c for every gap ω_i involved to get a critical line $k_c(\omega_i)$. Using a single $k_c(\omega_G)$ to approximate the critical line may affect the devil's staircase and therefore the $f(\alpha)$ spectrum. However, the critical exponents do not seem to be affected by this approximation.

ACKNOWLEDGMENTS

This work was supported in part by NSF grant DMR 89-02220. This work was completed while one of us (B.H.) was visiting the Institute of Physics of Academia Sinica in the summer of 1991. He would like to thank Dr. C. K. Hu for the invitation and the National Science Council for support. B.L. would like to thank Dr. P. H. Hor for summer support.

REFERENCES

1. Y. I. Frenkel and T. Kontorova, *Zh. Eksp. Teor. Fiz.* **8**:1340 (1938).
2. P. Bak, *Rep. Prog. Phys.* **45**:587 (1982).
3. G. Gruner, *Commun. Solid State Phys.* **10**:183 (1983).
4. I. E. Dzyaloshinskii, *Zh. Eksp. Teor. Fiz.* **46**:1420 (1964); *Sov. Phys. JETP* **23**:960 (1964).
5. M. S. Dresselhaus and G. Dresselhaus, *Adv. Phys.* **30**:139 (1981).
6. D. Schechtman, I. Blech, D. Gratios, and J. W. Cahn, *Phys. Rev. Lett.* **53**:1951 (1984).
7. F. Nabarro, *Theory of Crystal Dislocation* (Clarendon, Oxford, 1967).
8. S. C. Ying, *Phys. Rev. B* **3**:4160 (1971).
9. M. Toda, *J. Phys. Soc. Jpn.* **22**:431 (1967).
10. A. Milchev, *Phys. Rev. B* **33**:2062 (1986); A. Milchev and G. M. Mazzucchelli, *Phys. Rev. B* **38**:2808 (1988).
11. M. Peyrard and S. Aubry, *J. Phys. C* **16**:1593 (1983); S. Aubry, in *Proceedings of the Les Houches Lectures*, R. Balian and R. Stora, eds. (North-Holland, Amsterdam, 1981).
12. S. Aubry, *Physica* **7D**:240 (1983).
13. S. Aubry and P. Y. Le Daeron, *Physica* **8D**:381 (1983).
14. O. Biham and D. Mukamel, *Phys. Rev. A* **39**:5326 (1989).
15. H. J. Schellnhuber, H. Urbschat, and A. Block, *Phys. Rev. A* **33**:2856 (1986); H. J. Schellnhuber, H. Urbschat, and J. Wilbrink, *Z. Phys. B* **80**:305 (1990).
16. I. Niven, *Diophantine Approximations* (Wiley, New York, 1960).

17. I. Niven and H. S. Zuckerman, *An Introduction to the Theory of Numbers* (Wiley, New York, 1980).
18. S. Aubry, in *Solitons and Condensed Matter Physics*, A. R. Bishop and T. Schneider, eds. (Springer-Verlag, Berlin, 1979).
19. L. de Seze and S. Aubry, *J. Phys. C* **17**:389 (1984).
20. T. C. Halsey, M. H. Jensen, L. P. Kadanoff, I. Procaccia, and B. I. Shraiman, *Phys. Rev. A* **33**:1141 (1986).
21. J. M. Greene, *J. Math. Phys.* **20**:1183 (1979).
22. S. J. Shenker and L. P. Kadanoff, *J. Stat. Phys.* **27**:631 (1982).
23. J. M. Greene, R. S. Mackay, F. Vivaldi, and M. J. Feigenbaum, *Physica* **3D**:468 (1981).
24. H. Johannesson, B. Schaub, and H. Suhl, *Phys. Rev. B* **37**:9625 (1988).
25. R. S. MacKay, *Physica D* **50**:71 (1991).
26. J. Shi and B. Hu, *Phys. Rev. A* **45**:5455 (1992).
27. J. M. Greene, H. Johannesson, B. Schaub, and H. Suhl, *Phys. Rev. A* **36**:5858 (1987).